World Academy of Science, Engineering and Technology
International Journal of Urban and Civil Engineering
Vol:17, No:11, 2023

Analysis on Spatiotemporal Pattern of Land Surface Temperature in Kunming City, China

Jinrui Ren, Li Wu

Abstract**—**Anthropogenic activities and changes of underlying surface affect the temporal and spatial distribution of surface temperature in Kunming. Taking Kunming city as the research area, the surface temperature in 2000, 2010 and 2020 as the research object, using ENVI 5.3 and ArcGIS 10.8 as auxiliary tools, and based on the spatial autocorrelation method, this paper devoted to exploring the interactions among the changes of surface temperature, urban heat island effect and land use type, so as to provide theoretical basis and scientific basis for mitigating climate change. The results showed that: (1) The *heat island effect* was obvious in Kunming City, the high temperature area increased from 604 km^2 in 2000 to 1269 km^2 in 2020, and the sub-high temperature area reached 1099 km^2 in 2020; (2) In terms of space, the spatial distribution of LST was significantly different with the change of underlying surface. The high temperature zone extended in three directions: south, north and east. The overall spatial distribution pattern of LST was high in the east and low in the west. (3) The inter-annual fluctuation of land surface temperature (LST) was large, and the growth rate was faster, from 2000 to 2010. The lowest temperature in 2000 was 13.45 ℃, which raised to 19.71 ℃ in 2010, and the temperature difference in 10 years was 6.26 ℃. (4) The land use/land cover type has a strong effect on the change of LST: the man-made land made a great contribution to the increase of LST, followed by grassland and farmland, while forest and water have a significant cooling effect on LST. To sum up, the variation of surface temperature in Kunming is the result of the interactions of human activities and climate change.

Keywords**—**Surface temperature, urban heat island effect, land use cover type, spatiotemporal variation.

I. Introduction

As an important parameter of surface process variation, surface temperature plays an important role in the research field of global climate change, surface radiant energy balance, urban thermal environment, resource environment monitoring and so on [1]. At present, it is widely used in urban heat island effect [2], ecological environment assessment [3], climate change [4], vegetation monitoring [5] and many other fields. Since 1996, China's urbanization has entered a period of rapid development, with an average annual increase of 1.45%. The country's urban population had reached 666 million, with an urbanization rate of 49.68% [6]. With the continuous acceleration of urbanization, many impervious water surfaces dominated by cement, asphalt and other materials have destroyed the original land cover and natural landscape, and further caused changes in surface state parameters such as surface albedo and specific emissivity, thus breaking the surface heat balance and significantly changing the urban thermal environment. The change of urban thermal environment will not only reduce the comfort of human settlement, but also seriously affect the regional climate to a certain extent [7], [8].

The traditional method of acquiring LST data was through a single point of ground observation, but due to the limitation of the number and uneven distribution of weather stations, it was impossible to obtain large area LST data [9]. In recent years, thanks to the rapid development of remote sensing technology and geographic information system technology, the use of various thermal infrared sensors to monitor surface temperature has become the mainstream means to obtain surface temperature data. Compared with traditional methods, it has the advantages of fast speed, wide observation range and strong time continuity [10]. At the same time, the geographic information system (GIS) technology for processing MODIS data is also improving day by day, and the two are applied to the process of land use, cover change and surface temperature change, which provides technical support for the land-air dynamic monitoring.

At present, many domestic and foreign scholars have explored the change rules and influencing factors of LST from different time and space scales [11]-[13]. Que et al. used the atmospheric correction method to retrieve LST in Poyang Lake basin, analyzed the temperature distribution characteristics of the basin in different periods (wet period and dry period), studied the correlation between underlying surface parameters and surface temperature in different periods, and revealed the characteristics of temperature changes caused by changes in the properties of the underlying surface in Poyang Lake basin [14]. Chen et al. analyzed the characteristics of change in human activity intensity and LST on the north slope of Tianshan Mountains from 2000 to 2018, and they further explored the correlation between the two, and revealed that there was a significant positive correlation between the intensity of human activity and LST in the north slope of Tianshan Mountains, and the change scope of human activity and land use form would affect the regional differences and correlation [15]. Buya et al. chose Bali as the study area and identified five possible warming modes using quadratic polynomials. The logistic regression model evaluated the probability of warming [16]. Over the past 20 years, a quarter of Bali has warmed with the

This work was supported by the National Natural Science Foundation of China under grant no. 42161041, the Science and Technology planning Project of Yunnan Province, grant number 202305AC160089, and the Innovation and entrepreneurship training program for college students, grant number 202111390028.

Ren Jinrui is an undergraduate student at the School of Geography and Land Engineering, Yuxi Normal University, Yuxi 653100 China.

Li Wu is a professor at the School of Geography and Land Engineering, Yuxi Normal University, Yuxi 653100 China (corresponding author, e-mail: wuli2009@yxnu.edu.cn).

highest temperatures in urban and built-up areas and deciduous forests, where the temperature is inversely correlated with its altitude. Based on the remote sensing interpretation of MODIS LST products and TM images in the Tianshan Mountains from 2001 to 2013, Guan et al. analyzed the spatio-temporal characteristics of LST in the Tianshan Mountains and found that the LST in the Tianshan Mountains increased slowly year by year [17]. At present, the LST research in China has achieved a lot of research results [18], [19], but the research time span is short, the research sites are mainly concentrated in Beijing, Shanghai and other areas with obvious urban heat island effect, or Tianshan Mountains, Qinghai-Tibet Plateau and other areas with significant vertical climate differences. However, there are few studies on the southwest regions with complex topography and diverse climate types [20], [21], especially the analysis on the spatial-temporal pattern of surface temperature in Kunming region, which is vulnerable to ecological environment damage, needs to be studied.

Yunnan-guizhou Plateau, located in the southwest of China, is one of the four plateaus with a total area of about 5×10^5 km^2. The terrain is high in the northwest and low in the southeast, which resists the cold currents from Siberia. Kunming is located in the middle of the Yunnan-Guizhou Plateau, sheltered by the Yunnan-Guizhou Plateau. Since the cold air cannot reach the south, the annual temperature difference is small. The study of LST in Kunming City can not only explore the correlation between land use/land cover and LST, but also can provide reference for urban environmental planning and promote urban sustainable development. Therefore, to provide theoretical and scientific basis for mitigating climate change, this paper took Kunming as a research area, to explore the spatio-temporal changes of LST and the contribution of different land use types to LST.

II. Materials and Methods

A. Study Area

Kunming is in the central part of Yunnan Province and located between 102°10' to 103°40' east longitude and 24°23' to 26°22' north latitude. The area is 237.50 km long from north to south and 152 km wide from east to west, with a total area of 21012.54 km^2 [22]. Because it is in the Yunnan-Guizhou Plateau, the terrain is high in the north and low in the south, and gradually decreases from north to south in a ladder shape. Most of the area is between 1500 m and 2800 m above the sea level. The three sides of the city are surrounded by mountains and one side facing Dianchi Lake in the south.

Kunming is located in the intersection of China-ASEAN Free Trade area, Lancang-Mekong Cooperation area and pan-Pearl River Delta economic circle. It is an important gateway for China to South Asia, Southeast Asia and even the Middle East, Southern Europe and Africa, with the unique geographical advantages of "connecting Guizhou and Guangxi to the South China Sea in the east, Sichuan and Chongqing to the Central Plains in the north, Vietnam, Thailand and Cambodia in the south, and Myanmar to India and Pakistan in the west" [23] (Fig. 1).

B. Data Sources and Processing

The surface temperature data used in this paper come from LAADSDAAC, and the LST data of May each year are used as the research object. In the ArcGIS10.8 software, the temperature raster data are visualized, and the formula T = t + 273.15k is used to convert and calculate the temperature data in Kelvin (K) [24] and the temperature data in Celsius (°C) are obtained. The spatial-temporal change data of land use of Kunming city in 2000, 2010 and 2020 were derived from the land cover data provided by the website of http://www.globallandcover.com/ [25]. Based on the GIS spatial analysis method, the correlation between the spatial characteristics of ground classes and the surface temperature in Kunming city was comprehensively analyzed.

C. Methods

Spatial autocorrelation refers to the correlation of the same variable in different spatial locations, and is a measure of the aggregation degree of spatial unit attribute values [26]. As a spatial statistical method, its global and local spatial autocorrelation can describe the relationship between geographical things, and express the aggregation or discrete state among the attributes of spatial elements. According to the definition of spatial autocorrelation, it can be determined that urban hot (cold) island city is a spatial autocorrelation phenomenon, because urban heat island is an open system, which is affected by other regions while spreading to other regions [27], [28].

The spatial analysis module of ArcGIS10.8 was used to analyze the spatial autocorrelation. The formulas [29], [30] are as follows:

$$Global\ Moran's\ I = \frac{n\sum_{k=1}^{n}\sum_{l=1}^{n}\omega_{kl}(P_k - P_{mean})\times(P_l - P_{mean})}{\sum_{k=1}^{n}\sum_{l=1}^{n}\omega_{kl}\times\sum_{k=1}^{n}(P_k - P_{mean})^2} \tag{1}$$

$$Local\ Moran's\ I_k = \left[\frac{P_k - P_{mean}}{(\sum_{l=1,l\neq k}^{n} P_l^2)/(n-1) - P_{mean}^2}\right]\times\sum_{l=1}^{n}\omega_{kl}(P_k - P_{mean}) \tag{2}$$

where, P_k and P_l are the values of patch k and l respectively, ω_{kl} is the weight coefficient matrix, and n is the number of patches.

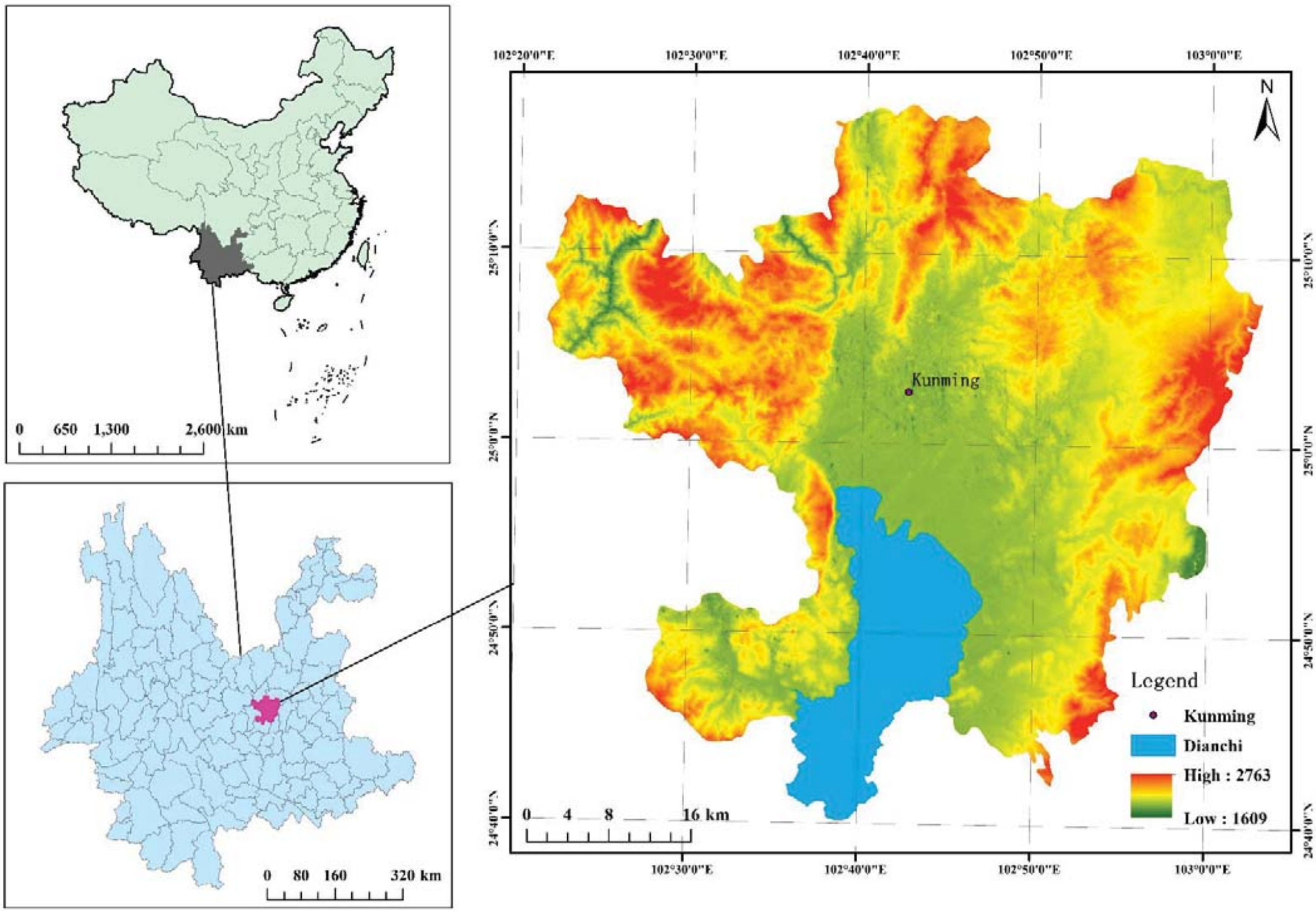

Fig. 1 Geographical location and elevation of the study area

III. Results and Analysis

A. Analysis on Temporal Variation of LST

To explore the changes of LST in different time and space scales, ArcGIS 10.8 was used to visualize the data. The natural discontinuity point classification method was used to classify LST into four categories: the low temperature zone (below 25 ℃), the secondary low temperature zone (26-30 ℃), the secondary high temperature zone (31-35 ℃), and the high temperature zone (above 35 ℃) (Fig. 2).

As can be seen from Fig. 2, there were obvious differences in surface temperature in Kunming in the past three years. The abrupt line of low temperature roughly overlapped with the water body boundary, and the surface temperature showed an overall upward trend. The high temperature area showed a trend of spreading around, increasing from 604 km^2 in 2000 to 833 km^2 in 2010. By 2020, the high temperature area reached 1269 km^2, and its spatial pattern also changed significantly. In 2000, the high temperature center was obviously clustered in the south of Wuhua District. From 2000 to 2010, the temperature increased obviously, and the high temperature area was distributed along the east bank of Dianchi Lake, and a new high temperature center appeared.

From 2010 to 2020, the temperature growth rate slowed down, but the high temperature region was still expanding to the periphery, the high temperature region was expanding, and so was the number of high temperature centers, the regional differences were further increasing. In 2000, the sub-high temperature area mainly concentrated in the eastern and northern Dianchi basin. By 2010, the sub-low temperature region in the west was gradually replaced by the sub-high temperature region, and there was a trend of advancing to the northwest region. Due to the gradual expansion of the high temperature area and the sub-high temperature area into the neighborhood, the high temperature area became the largest in 2020, with an area of 1 269 km^2, followed by the sub-high temperature area, with an area of 1099 km^2. During the study period, the sub-low temperature area showed an obvious decreasing trend, from 698 km^2 in 2000 to 139 km^2 in 2020. Compared with other classification areas, the overall variation of low temperature area was small. Among them, the change amplitude between 2000 and 2010 was more significant than that between 2010 and 2020. During the 10 years, from 2010 to 2020, the decrease rate of low temperature area slowed down, and there was a slight trend of growth.

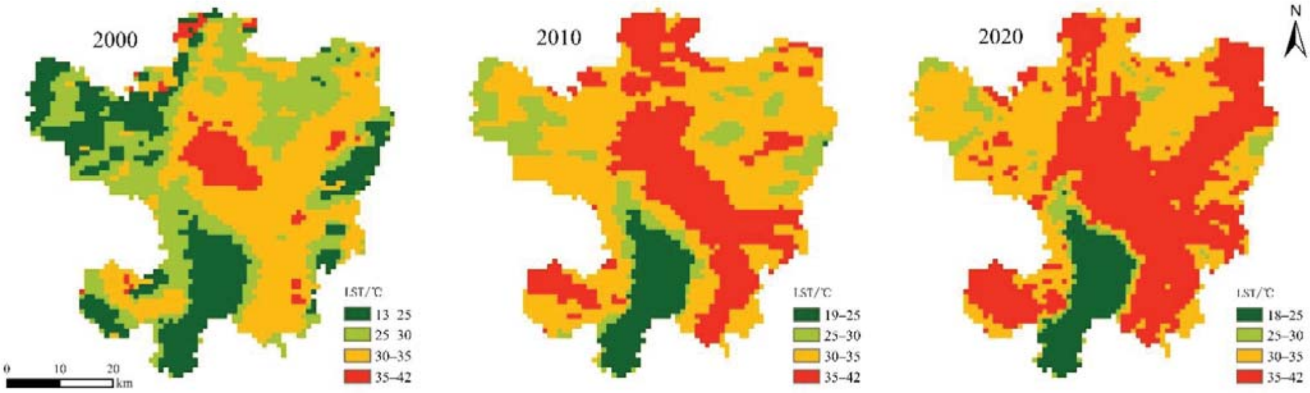

Fig. 2 Spatial distribution of LST in Kunming City

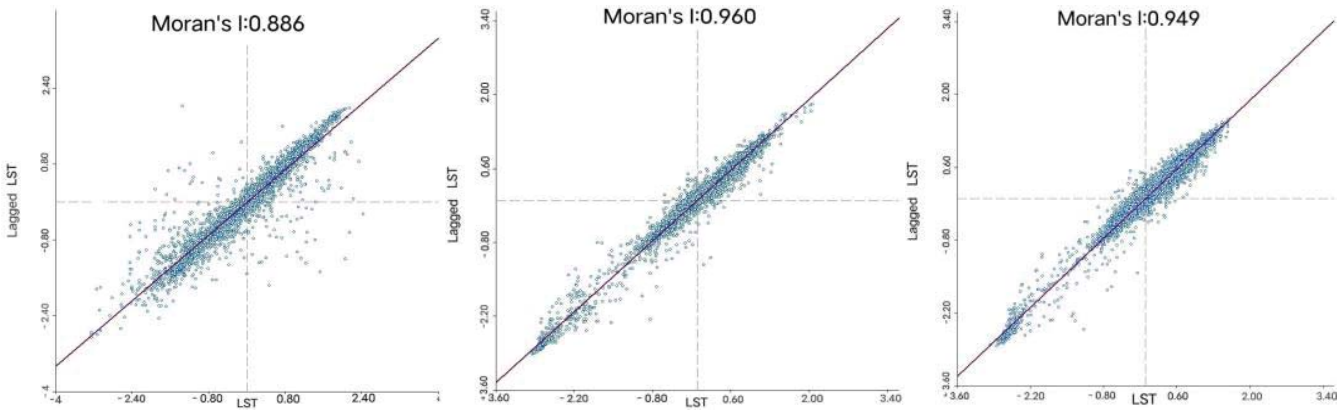

Fig. 3 Moran's I index of the LST in Kunming City

B. *Spatial Statistical Analysis of Surface Temperature*

The Rook spatial weight matrix was created in Geoda, the global Moran index of each year was calculated through the spatial analysis module and the significance of the index values was tested, and the global Moran's I scatter plot of LST was shown in Fig. 3. As shown in the figure, the Moran's I index of LST of Kunming in 2000, 2010 and 2020 was 0.866, 0.960 and 0.949, respectively, and the Moran's I were all greater than 0 and close to 1, indicating that the LST in these three years showed significant spatial autocorrelation [31]. From the global Moran's I value, it can be found that the Moran's I value increased, indicating that the concentration distribution of surface temperature in Kunming has become more and more intense.

From the perspective of global autocorrelation analysis, there was spatial agglomeration of surface temperature in Kunming, but the global spatial autocorrelation cannot reflect the spatial characteristics of the study area. Based on this, it is necessary to construct a local spatial Molan index model for further analysis and show the spatial agglomeration characteristics of LST in Kunming through the LISA agglomeration map. The cluster analysis tool in ArcGIS tool module was used to obtain LISA cluster maps for 2000, 2010 and 2020, which can visualize the spatial pattern. LISA clusters were divided into five colors, representing different association types, denoted by "high-high", "high-low", "low-high", "low-low" and "not significant" (Fig. 4).

TABLE I
LOCAL SPATIAL AUTOCORRELATION TYPES OF LST IN KUNMING CITY

Type	2000		2010		2020	
	Number	Proportion /%	Number	Proportion /%	Number	Proportion /%
H-H	708	21.51	784	24.27	762	23.68
H-L	9	0.26	0	0	0	0
L-H	3	0.09	0	0	0	0
L-L	653	20.20	375	11.61	372	11.51
NOT	1875	58.03	2071	64.12	2096	64.81
SUM	3230	100.00	3230	100.00	3230	100.00

According to Fig. 4 and Table I, the "high-high" type area accounted for 21.51%, 24.27% and 23.68% of the study area, respectively. In 2000 and 2010, Panlong District, Chenggong District and Guandu District mainly belonged to the "high-high" type area, showing a trend of north-south extension distribution around Guandu District. In 2010, the southern part of the Xishan District expanded and gathered in a cluster. In 2020, this type conversion transmitted from Guandu District to Chenggong District, adding a new cluster center in the north of Wuhua District. Overall, the "high-high" area increased, due to the acceleration of urbanization, the relatively flat terrain of the city center, and the boom in modernization, resulting in an increase in artificial surface area. There were even several areas where the arable land is zero.

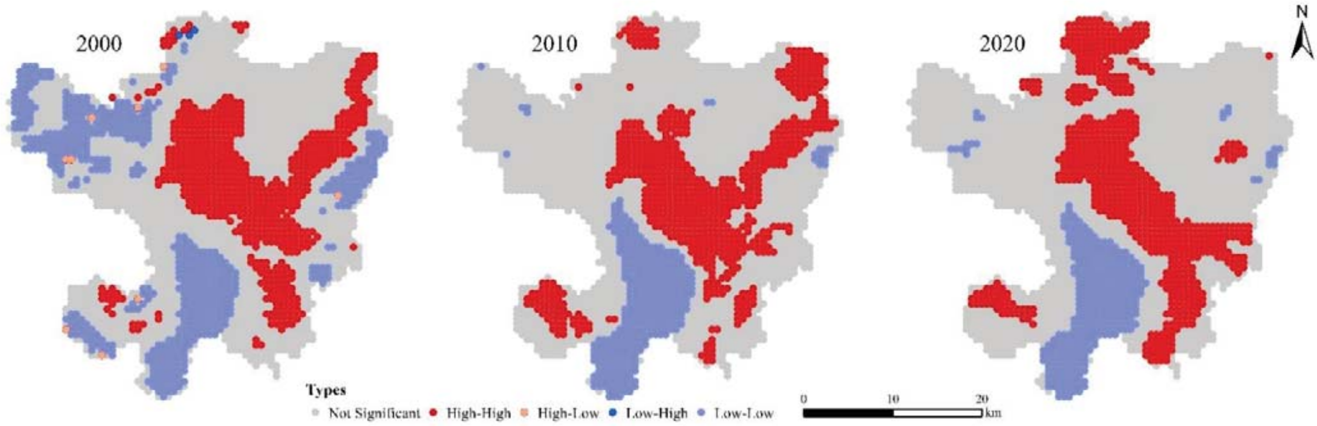

Fig. 4 Local spatial autocorrelation distribution of the LST in Kunming City

The "low-low" type area showed a decreasing trend during the study period. In 2000, this type of area accounted for about 20%, and the decrease rate accelerated in the later period, accounting for only 11.61% and 11.51% in 2010 and 2020, respectively. In 2010 and 2020, the northern part of the Xishan District changed from "no significant" area to "low-low" type area. In 2010, the "low-low" type expanded in the Dianchi basin, but there was little change in other areas, and it was still an "insignificant" type area.

In 2000, there were nine "high-low" type areas, accounting for about 0.26%, and most of them were located near the "low-low" type areas in the Xishan District, where the number of green plants was large. However, with the development of the city, there were not such types of area since 2010, and it has been transformed into an "insignificant" type, and the spatial correlation decreased. In 2000, there were only 3 "low-high" type areas, accounting for about 0.09%, all located in the north of Wuhua District, near the "high-high" type area. By 2010, such areas had disappeared and turned into "high-high" types, which had nearly doubled in size by 2020.

C. *Influencing Factors of LST Spatio-Temporal Changes*

Effect of Elevation on Surface Temperature

LST and altitude were significantly negatively correlated, and LST decreases with elevation increase. Each 100 m elevations increase, temperature decreases by 0.6 °C. As shown in Fig. 1, the redder the color, the higher the altitude, and the bluer the color, the lower the altitude. That is, the highest altitude in the main urban area is 2763 m, the lowest is 1609 m, and the difference of altitude is 1 154 m. To verify whether the relationship between altitude and surface temperature in Kunming conforms to this principle, the bivariate correlation tool was used in SPSS software to confirm the correlation between the two (Fig. 5). The surface temperature represented by the vertical coordinate showed a slow increase trend with the decrease of altitude represented by the horizontal coordinate, which conforms to the principle.

Due to the difference in specific heat capacity, the temperature of the area covered by water changed more slowly than the area without water cover, resulting in the difference in ground temperature. Except for the Dianchi Lake basin, elevation and temperature in other regions showed a negative correlation during the three years. The terrain was high in the surrounding areas and low in the middle, so the LST in the central and southern areas was lower than that in the surrounding areas, the temperature decreased with the increase of altitude, and the vertical differentiation of LST was obvious. Among them, the northern Xishan District and the eastern Guandu District were high-altitude accumulation areas. By 2010, the low temperature zone disappeared, and only the secondary low temperature zone remained, with its area decreasing. The temperature distribution showed a significant geomorphic feature, from the central (except water) to the north and east, the temperature decreased with the increase of altitude. The surface temperature in the eastern part of the central region was higher than that in the western region, which showed a certain cross-distribution characteristic overall and was consistent with the trend of the mountains.

Effect of Land Use/Cover Type on LST

The surface temperature of different land types was different, and the surface temperature of the same land type was also different in different research periods [32]. The statistical data show that the average surface temperature of different land use types in three years is the highest in construction land and the lowest in water area (Table II) in three years. The changes of LST and land use/land cover in 2000, 2010 and 2020 were basically consistent. The area with low surface temperature was mainly in the area with higher elevation in Kunming City, and covered by forest and grass. The green vegetation of these two types of land was abundant, and vegetation can absorb carbon dioxide in the atmosphere through photosynthesis, thereby reducing the concentration of carbon dioxide in the atmosphere and the ambient temperature. Therefore, the superimposed effects of altitude and land cover type can reduce LST.

Among all land classes, water body was also the typical low-temperature land class. The area with low temperature in Kunming was mainly concentrated in the Dianchi Basin. The average temperature of water body in 2000, 2010 and 2020 is 24.39 °C, 23.25b°C and 22.47 °C respectively, and the annual temperature difference changes were small. Due to the difference in heat capacity between the water body and the surrounding ground, the LST in the surrounding area heated up faster under sunlight, and the air flow was heated up. Due to the large heat capacity and slow temperature rising, the water temperature was lower than that of the surrounding areas, and the airflow shrinks and sinks, forming a local microclimate. Therefore, the three-year LST classification map showed that the LST of the water body and the surrounding ground belonged to the low temperature area and the sub-low temperature area, and the "cold island effect" was obviously shown.

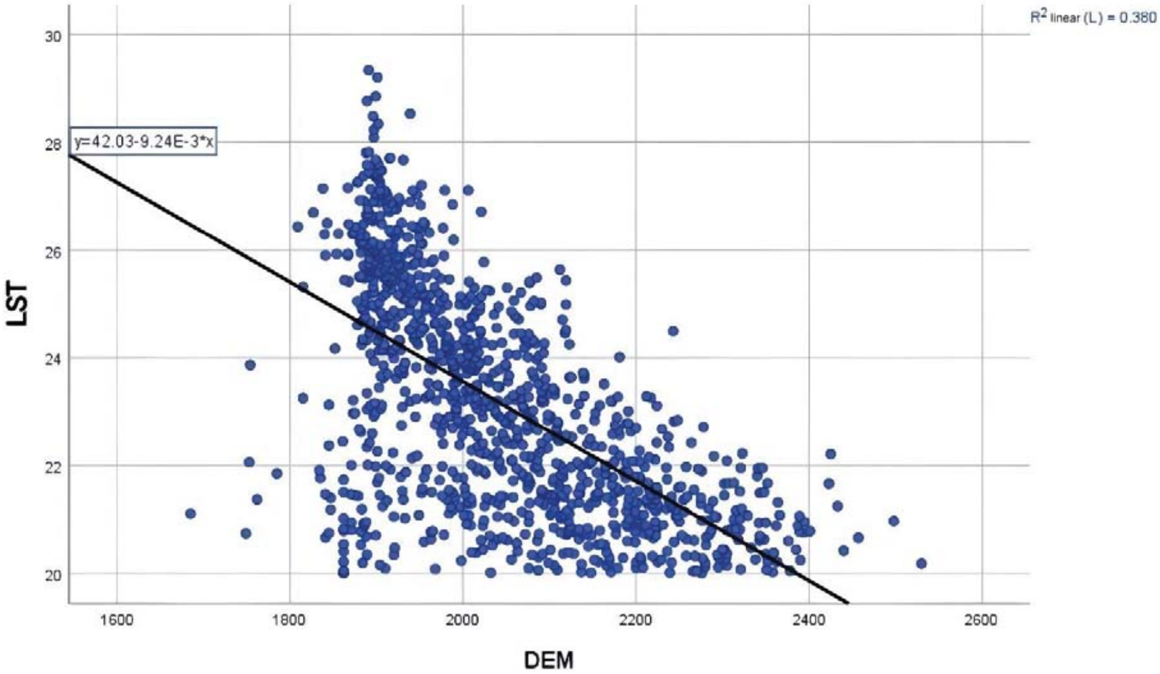

Fig. 5 Correlation between elevation and LST in Kunming city

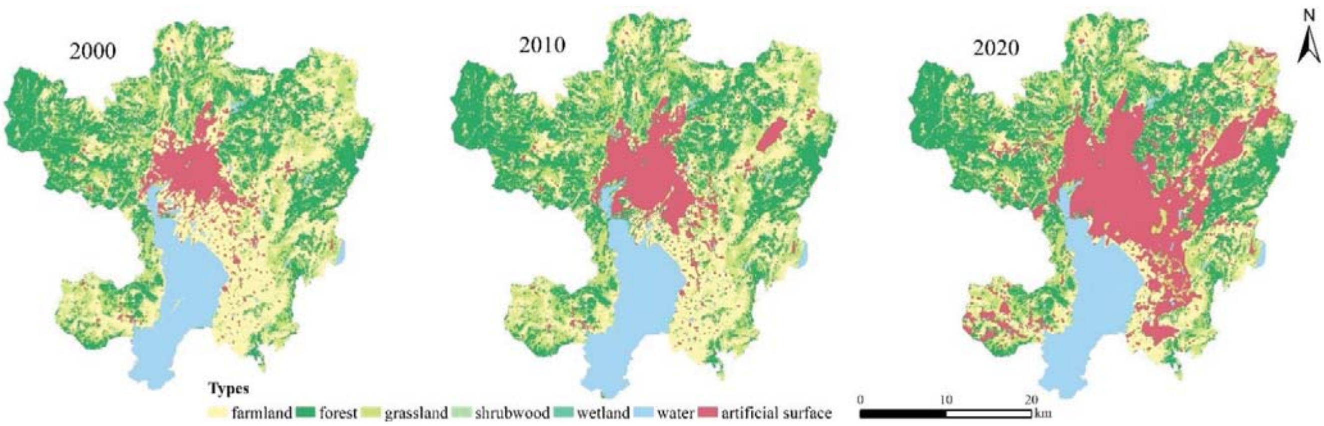

Fig. 6 Spatial distribution of land use/land cover in Kunming City

However, LST of the land use type dominated by artificial land surface was significantly higher than that of other land use types, and was always the highest (34.7 °C, 35.42 °C and 37.2 °C, respectively), indicating that its underlying surface changed dramatically. The artificial surface was mainly covered by impervious layers (such as cement hardened pavement and building roof), and its material structure had low water content, low surface latent heat capacity and high thermal conductivity. After receiving solar radiation, the surface temperature rises very fast. In addition, on the land of urban building, commercial and residential areas were the most widely distributed. In these areas, population density is high, economic and social activities are frequent, and man-made heat emissions are large, which is also a major factor leading to high surface temperature [33].

In summary, LST of different land use types was significantly different. The farmland and artificial land surface were positively correlated with its surface temperature, while forest, grassland, shrubwood, wetland and water body were negatively correlated with its surface temperature.

The significant differences in the changes of LST in the study area in 2000, 2010 and 2020 were due to the difference in land use/cover type from year to year (Fig. 6). To reveal the change characteristics of LST in different land use/land cover types, based on the overlapping of graded LST data with ArcGIS 10.8, the intersection data were derived and the statistical tables of LST and LUCC of Kunming in different years were sorted out (Table II). The data in the table clearly showed the land classes covered by each temperature range and the area of the land classes in the study area in different periods, which can further explore the correlation between the changes of LST and LUCC in the study area in the past 20 years. From 2000 to 2010, the surface temperature increased, the area of high temperature and low temperature increased, and that of low temperature decreased. During these 10 years, the area of farmland and water body showed a decreasing trend. The farmland decreased by 153 km^2, with a change rate of 17.04%. LST increased by 3.63 ℃ on average, while water body decreased by 16.63 km^2, with a reduction rate of 5.16%, and LST decreased by 1.14 ℃ on average. The forest, grassland, shrub land, wetland and artificial surface showed an increasing trend, in which the artificial surface increased the most, and the wetland increased the least, but the change rate of wetland was higher than that of artificial surface, because the wetland area in the study area was small and the changing part accounted for a large proportion of the total wetland area. While the area of these land types increased, the surface temperature also changed and showed an increasing trend. From 2010 to 2020, the high temperature area increased continuously, while the low temperature area and the sub-low temperature area decreased. By 2020, the low-temperature zone, except for water basins, will have less area in the low-temperature zone and will be replaced by high temperature and sub-high temperature zones. In the past 10 years, except for the increase of artificial surface and water, the other cover types showed a decreasing trend. The artificial surface increased rapidly from 291.75 km^2 in 2010 to 664.59 km^2 in 2020, with a change rate as high as 127.79%. During the ten years from 2000 to 2010, the artificial surface temperature increased by 0.72 ℃, and from 2010 to 2020 by about 1.78 ℃. LST growth rate was about twice that of the previous ten years, mainly due to the rapid development of social economy, rapid population growth, urban construction, increasing demand for land, and limited land resources.

TABLE II
STATISTICS OF LAND USE AREA IN DIFFERENT TEMPERATURE REGIONS OF KUNMING CITY IN 2000, 2010 AND 2020

Year	low temperature zone		secondary low temperature zone		secondary high temperature zone		high temperature zone	
	type	area/km^2	type	area/km^2	type	area/km^2	type	area/km^2
2000	farmland	85.80	farmland	245.02	farmland	519.47	farmland	39.90
	forest	267.83	forest	362.64	forest	181.98	forest	9.48
	grassland	79.26	grassland	166.44	grassland	209.77	grassland	10.83
	shrubwood	2.13	shrubwood	4.91	shrubwood	13.52	shrubwood	0.96
	wetland	0.40	wetland	0.83	wetland	0.17	—	—
	water	236.09	water	60.31	water	21.95	water	0.10
	artificial surface	1.97	artificial surface	13.66	artificial surface	106.83	artificial surface	97.33
2010	farmland	5.70	farmland	51.42	farmland	392.57	farmland	287.35
	forest	1.52	forest	185.76	forest	540.75	forest	130.02
	grassland	0.53	grassland	25.71	grassland	323.67	grassland	161.31
	shrubwood	0.07	shrubwood	1.13	shrubwood	16.16	shrubwood	10.58
	wetland	0.91	wetland	1.62	wetland	0.80	wetland	1.51
	water	240.18	water	36.49	water	21.59	water	3.31
	artificial surface	0.95	artificial surface	9.51	artificial surface	60.75	artificial surface	220.48
2020	farmland	4.24	farmland	14.35	farmland	199.94	farmland	289.02
	forest	0.41	forest	67.20	forest	576.07	forest	159.23
	grassland	0.22	grassland	13.05	grassland	215.65	grassland	201.94
	shrubwood	0.06	shrubwood	0.43	shrubwood	5.40	shrubwood	11.05
	wetland	0.20	wetland	0.30	wetland	0.37	wetland	0.02
	water	250.37	water	33.07	water	17.95	water	8.46
	artificial surface	0.82	artificial surface	6.94	artificial surface	65.11	artificial surface	589.83

Combined with Fig. 2 and Table II, the changes in LST and land use/cover type change showed a high degree of spatial consistency. The regions with high perennial temperature were mainly concentrated in the foothills, which were dominated by artificial surface and the perennial LST was above 30 ℃. The low temperature area of surface temperature was mainly concentrated in the water body type area in the central and southern part of the country. The annual average temperature was lower than 25 ℃, and it was in the range of 13 ℃-25 ℃. In addition to the above high temperature and low temperature areas, the temperature in other areas was between 25-35 ℃ for many years. In 2000, the high temperature area was clumped, mainly concentrated in the north of the water body, the land use type was mainly artificial surface, and the urban heat island effect was significantly enhanced. The west of the high temperature concentration area showed the cross distribution of the low temperature area and the secondary low temperature area, and the coverage type was mainly forest. The forest coverage rate was high, which weakened the direct irradiation of solar radiation on the ground, reduced the reflectivity, weakened the evaporation, and the ground temperature was not strong, so that this area became a low temperature area. The southern water body belonged to the low temperature area, which is the most prominent area of urban cold island effect (consistent with 2010 and 2020, no longer analyzed).

In 2010, there was a surge in the high temperature zone, extending from the clumps of 2000 to a north-south trending band of high temperature zone. The high temperature area is mainly distributed in the sub-high temperature area. Compared with 2000, the sub-high temperature area has increased towards the west. The land use type is mainly farmland, and the reflectance of the ground increases significantly. Due to the small specific heat of sand and gravel, the temperature of the ground increases rapidly under sunlight during the day. In addition, the area of farmland decreases, the exposed ground increases, and the degree of urban heat island effect is deepened, and the influence scope is getting larger and larger.

With the passing of time, the heat island range of the study area showed a continuous increasing trend during the study period, expanding from the high temperature area in 2010 to the north and east. A new banded extension area in the high temperature area to the northeast appeared in 2020, and the urban heat island effect became more obvious. During this period, the artificial surface area increased and was mainly distributed in the high temperature region. Therefore, the main reason for the deterioration of the heat island effect was the expansion of artificial surface, the increase of impervious water surface and the enhancement of evaporation. Meanwhile, the decrease of farmland, forest, grassland, shrub-wood and wetland would change the vegetation cover on the surface, and the decrease of vegetation cover and biomass would also occur. This inevitably leaded to the weakening of photosynthesis, the less the amount of carbon dioxide absorbed by vegetation, the more the atmospheric carbon dioxide concentration, and the consequent warming of LST, further aggravating the urban heat island.

IV. Conclusions

Taking Kunming city as the research area, this paper elucidated the characteristics of LST change in 2000, 2010 and 2020. This paper devoted to exploring the relationship between the changes of LST and urban heat island effect and land use type, and drew the following conclusions:

1. There was an obvious urban heat island effect in Kunming, and the high temperature area was mainly distributed in the eastern area of the water basin with low green vegetation coverage, which was mainly man-made surface coverage type. The low temperature area has little inter-annual variations, mainly in the Dianchi Lake water basin, and the other areas were between the low temperature area and the high temperature area.
2. During the 20 years from 2000 to 2020, the surface temperature in Kunming showed a trend of overall increase in the range of high temperature area and sub-high temperature area, while the range of low temperature area continued to shrink.
3. The changes of different temperature zones in Kunming are consistent with the changes of land use/land cover type. With the development of urbanization, the sub-high temperature area and high temperature area in Kunming city appear fragmentation phenomenon.
4. The green construction in Kunming city is decreasing, although the proportion of the reduced part in the total area is low, but the urban heat island problem remains serious, mainly because of the prominent urban overflow. Therefore, in the future, urban development should be scientifically planned, population and building density should be controlled, and greening rate should be selectively improved, so as to achieve a balanced development of economy, society and ecology.

References

[1] Y. N. Li, "Discussion on land surface temperature inversion based on Landsat 8 imagery," Journal of Earth Environment, vol. 32, no. 5, pp. 238-239, 2020.
[2] H. F. Guo, C. Zhang, and S. Cao, "Research status of urban heat island effect," Agriculture and Technology, vol. 42, no. 10, pp. 113-115, 2022.
[3] C. B. Chen, J. Peng, and G. Y. Li, "Evaluating ecosystem health in the grasslands of Xinjiang," Arid Zone Research, vol. 39, no. 1, pp. 270-281, 2022.
[4] X. Ren, Z. G. Shi, "Response of global temperature extremes in mid-Holocene: results from MPI-ESM-P experiments," Journal of Earth Environment, vol. 10, no. 5, pp. 465-478, 2019.
[5] Z. Sun, "The Temporal-Spatial Distribution and Driving Mechanism of Changes of Vegetation Carbon Source/Sink in the Three Gorges Reservoir Area," Chongqing University, 2021.
[6] "Key Data Bulletin of the Sixth National Population Census 2010 (No. 1)," Chinese Journal of Family Planning, vol. 19, no. 08, pp. 511-512, 2011.
[7] C. Y. Yin, Y. S. Shi, and H. F. Wang, et al. "Impacts of urban landscape form on thermal environment at multi-spatial levels," Resources and Environment in the Yangtze Basin, vol. 24, no. 1, pp. 97-105, 2015.
[8] W. H. Kuang, "Advance and Future Prospects of Urban Land Use/Cover Change and Ecological Regulation of Thermal Environment," Scientia Geographica Sinica, vol. 38, no. 10, pp. 1643-1652, 2018.
[9] H. W. Liang, Alimujiang Kasmu, H. M. Zhao, and Y. Y. Zhao, "The surface temperature and its influencing factors in Urumqi City based on the geodetector," Journal of Lanzhou University (Natural Sciences), vol. 58, no. 3, pp. 356-363, 2022.
[10] R. Luo, "Towards the Retrieval Methods for Land Surface Temperature in Urban Areas," University of Electronic Science and Technology of China, 2020.
[11] N. Wang, J. Y. Chen, T. He, X. L. Wu, L. Liu, Z. Y. Sun, Z. Qiao, D. R. Han, “Understanding the differences in the effect of urbanization on land surface temperature and air temperature in China: insights from heatwave and non-heatwave conditions,” Environmental Research Letters, vol. 18, no. 10, pp. 4038, 2023.
[12] M. Kim, D. Kim, G. Kim, “Examining the Relationship between Land Use/Land Cover (LULC) and Land Surface Temperature (LST) Using Explainable Artificial Intelligence (XAI) Models: A Case Study of Seoul, South Korea,” International Journal of Environmental Research and Public Health, vol. 19, no. 23, pp. 15926-15926, 2022.
[13] M. He, Y. M. Xu, Y. P. Mo, S. Y. Zhu, “Assessment of heat wave risk in Beijing using multi-source remote sensing data,” Scientia Geographica Sinica, vol. 43, no. 7, pp. 1270-1280, 2023.
[14] Y. Y. Que, X. Y. Hu, S. L. Wang, S. Y. Lin, D. F. Lu, “The spatio-temporal difference between underlying surface parameters and surface temperature: a case study of Poyang Lake basin,” Journal of Hunan City University (Natural Science), vol. 31, no. 4, pp. 36-43, 2022.
[15] H. J. Chen, L. Liu, Z. Y. Zhang, et al. “Spatiotemporal correlation between human activity intensity and surface temperature on the north slope of Tianshan Mountains,” Acta Geographic Sinica, vol. 77, no. 5, pp. 1244-1259, 2022.
[16] S. Buya, C. C. Potjamas, A. O. Benjamin, “Analysis of land surface temperature with land use and land cover and elevation from NASA MODIS satellite data: a case study of Bali, Indonesia,” Environmental Monitoring Assessment, vol. 194, no. 8, pp. 566, 2022.
[17] T. L. Guan, R. H. Wang, C. Li, J. Yao, M. Zhang, J. P. Zhao, "Spatial-temporal characteristics of land surface temperature in Tianshan Mountains area based on MODIS data," Chinese Journal of Applied Ecology, vol. 26, no. 3, pp. 681-688, 2015.
[18] F. F. Zhang, K. Peng, F. Zhang, “Spatial distribution characteristics of

land surface temperature and its "source-sink" effect in Yanqi Basin, Xinjiang," Transactions of the Chinese Society of Agricultural Engineering, vol. 38, no. 16, pp. 153-161, 2022.
[19] E. L. Zhao, F. Deng, Z. Y. Li, P. X. Zheng, F. Qian, Y. Han, "Study on the thermal environment of Wuhan City based on local climate zones," Resources and Environment in the Yangtze Basin, vol. 32, no. 5, pp. 1030-1041, 2023.
[20] L. G. Kang, S. K. Cao, G. C. Cao, L. Yan, L. X. Chen, W. B. Li, H. R. Zhao, "Spatiotemporal variation of land surface temperature in Qinghai Lake Basin," Arid Land Geography, vol. 46, no. 7, pp. 1084-1097, 2023.
[21] Y. Luo, W. F. Peng, Y. B. Dong, Y. M. Luo, D. M. Zhang, "Geographical exploration of the spatial pattern of the surface temperature and its influencing factors in western Sichuan Plateau: A case of Xichang City," Arid Land Geography, vol. 43, no. 3, pp. 738-749, 2020.
[22] J. Shi, X. Y. Lu, X. Chen, "Study on the impact of urbanization and urban heat island effect on net primary productivity in Kunming," Pratacultural Science, vol. 39, no. 12, pp. 2589-2603, 2022.
[23] Edited by Office of Kunming Local Chronicles Compilation Committee. Kunming Yearbook. 2021, Nationalities Publishing House of Yunnan, 2021.
[24] K. G. Ying, "Kelvin-a versatile and prolific scientist," Physics Teaching, no. 2, 1984.
[25] X. H. Zhang, "Integrate Global Land Cover Products to Refine the Forest Type of Globe Land 30," Beijing University of Civil Engineering and Architecture, 2018.
[26] X. F. Wei, J. P. Wu, "Development and Research of Spatial Autocorrelation Based on ArcGIS," Geomatics & Spatial Information Technology, pp. 672-680, 2004.
[27] W. Zhang, J. G. Jiang, Y. B. Zhu, "Spatial-temporal evolution of urban thermal based on spatial statistical features," Chinese Journal of Applied Ecology, vol. 26, no. 6, pp. 1840-1846, 2015.
[28] P. L. Wang, J. M. Zhang, R. F. Lv "Urban thermal environment pattern with spatial autocorrelation in Lanzhou," Chinese Journal of Ecology, vol. 33, no. 4, pp. 1089-1095, 2014.
[29] X. Y. Chen, P. Lin, "Spatial Autocorrelation Analysis on the Distribution of Mangrove in China," Journal of East China Normal University (Natural Science), no. 3, pp. 104-109, 2000.
[30] B. Meng, J. F. Wang, W. Z. Zhang, X. H. Liu, "Evaluation of Regional Disparity in China Based on Spatial Analysis," Scientia Geographica Sinica, vol. 25, no. 4, pp. 393-400, 2005.
[31] Z. G. Li, M. Y. Wang, J. Q. Niu, et al. "Analysis of the Spatial Pattern Evolution of Cultivated Land in Municipalities Based on Spatial Autocorrelation Analysis—Luoyang City as an Example," Journal of Xinyang Normal University (Natural Science Edition), vol. 34, no. 3, pp. 415-421, 2021.
[32] H. M. Zhou, F. Dong, "Research on Response of Land Use and Surface Temperature in Nan'an District of Chongqing City," Journal of Anhui Agricultural Sciences, vol. 49, no. 15, pp. 79-84, 2021.
[33] J. H. Ye, Y. W. Han, "Spatiotemporal dynamic analysis of surface temperature in Xiongan New Area from 2000 to 2019," Environmental Ecology, vol. 5, no. 2, pp. 5-12, 2023.